Searching for the fastest dynamo: Laminar ABC flows

Alexandros Alexakis

Laboratoire de Physique Statistique de l'Ecole Normale Supérieure, UMR CNRS 8550, 24 Rue Lhomond, F-75006 Paris Cedex 05, France

The growth rate of the dynamo instability as a function of the magnetic Reynolds number R_M is investigated by means of numerical simulations for the family of the Arnold-Beltrami-Childress (ABC) flows and for two different forcing scales. For the ABC flows that are driven at the largest available length scale, it is found that, as the magnetic Reynolds number is increased: (a) The flow that results first in a dynamo is the $2\frac{1}{2}$-dimensional flow for which $A = B$ and $C = 0$ (and all permutations). (b) The second type of flow that results in a dynamo is the one for which $A = B \simeq 2C/5$ (and permutations). (c) The most symmetric flow, $A = B = C$, is the third type of flow that results in a dynamo. (d) As R_M is increased, the $A = B = C$ flow stops being a dynamo and transitions from a local maximum to a third-order saddle point. (e) At larger R_M, the $A = B = C$ flow reestablishes itself as a dynamo but remains a saddle point. (f) At the largest examined R_M, the growth rate of the $2\frac{1}{2}$-dimensional flows starts to decay, the $A = B = C$ flow comes close to a local maximum again, and the flow $A = B \simeq 2C/5$ (and permutations) results in the fastest dynamo with growth rate $\gamma \simeq 0.12$ at the largest examined R_M. For the ABC flows that are driven at the second largest available length scale, it is found that (a) the $2\frac{1}{2}$-dimensional flows $A = B$, $C = 0$ (and permutations) are again the first flows that result in a dynamo with a decreased onset. (b) The most symmetric flow, $A = B = C$, is the second type of flow that results in a dynamo. It is, and it remains, a local maximum. (c) At larger R_M, the flow $A = B \simeq 2C/5$ (and permutations) appears as the third type of flow that results in a dynamo. As R_M is increased, it becomes the flow with the largest growth rate. The growth rates appear to have some correlation with the Lyapunov exponents, but constructive refolding of the field lines appears equally important in determining the fastest dynamo flow.

I. INTRODUCTION

Magnetic dynamo is the process through which an electrically conducting fluid amplifies and maintains magnetic energy against Ohmic dissipation by continuously stretching and refolding the magnetic field lines [1,2]. This process is considered to be the main mechanism for the generation of magnetic energy in the universe. It is present in the intergalactic and interstellar medium, in accretion disks, and in the interiors of stars and planets. Recently, it has also been realized in different laboratory experiments [3–5]. The flows in these examples vary in structure, and the generated magnetic fields exhibit a large variety of structural and temporal behaviors. It is then desirable to understand which properties of a flow are important for the amplification of magnetic energy and how do they effect the dynamical behavior of the magnetic field. This question is of particular interest for the dynamo experiments for which optimizing the flow is important for achieving a dynamo at small energy injection rates [6].

In theoretical studies, various flows have been examined analytically and numerically both in the laminar and in the turbulent regimes. The Ponomarenko [7], the ABC [8–10], the Roberts [11,12], the Taylor-Green [13], the cat's-eye [14], and the Archontis flows [15] are some of the flows that have been shown to result successfully in dynamo action provided that the magnetic Reynolds number R_M (the ratio of the large-scale velocity time scale to the large-scale diffusivity time scale) is sufficiently large. The choice of flow for study was motivated either by its similarity to astrophysical flows or due to its simplicity that allowed analytical treatment or made the investigation more tractable numerically. Other than this

practical motivation, there is no mathematical justification for preferring one flow over another.

This lack of mathematical reasoning motivates this paper. Across a family of flows of finite energy and vorticity, not all members are as efficient in producing dynamo action. Then, it is expected that a flow in this family exists that is optimal for dynamo action. Finding and investigating the properties of such an optimal flow can then reveal which mechanisms are important for magnetic field amplification. How an optimal flow is defined is described in the next section where the general problem is formulated in detail.

II. FORMULATION

At the early stages of the dynamo, when the Lorentz force is too weak to act back on the flow, the evolution of the magnetic field is given by the linear advection diffusion equation,

$$\partial_t \mathbf{b} + \mathbf{u} \cdot \nabla \mathbf{b} = \mathbf{b} \cdot \nabla \mathbf{u} + \eta \nabla^2 \mathbf{b}, \tag{1}$$

where $\mathbf{b}$ is the magnetic vector field, $\mathbf{u}$ is the velocity field, and η is the magnetic diffusivity. The advection term on the left hand side of Eq. (1) is responsible for the mixing of the magnetic field lines. The first term on the right hand side is the stretching term that is responsible for the increase in the magnetic energy while the last term is responsible for the destruction of magnetic energy due to diffusion. Since the equation for the magnetic field is linear, it expected that, after some transient behavior, the amplitude of the magnetic field will grow or will decay at an exponential rate,

$$\mathbf{b} \sim \tilde{\mathbf{b}}(\mathbf{x},t) e^{\gamma t}, \tag{2}$$

where γ is the growth rate and $\tilde{\mathbf{b}}$ is a bounded function in time. For steady velocity fields that will be examined here, $\tilde{\mathbf{b}}$ is either time independent or a periodic function of time.

The growth rate γ and its dependence on the flow parameters is the primary interest in this paper. Given the functional shape of $\mathbf{u}$, the only control parameter in the system is the magnetic Reynolds number R_M that, in this paper, is defined as

$$R_M \equiv \frac{U}{\eta k_u}. \tag{3}$$

η is the magnetic diffusivity. U is the amplitude of the velocity field that is defined as

$$U \equiv \langle \mathbf{u} \cdot \mathbf{u} \rangle^{1/2}, \tag{4}$$

where the angular brackets stand for spatial average. k_u is the velocity inverse length scale that we define through the vorticity of the flow $\mathbf{w} = \nabla \times \mathbf{u}$ as

$$k_u \equiv \langle \mathbf{w} \cdot \mathbf{w} \rangle^{1/2}/U. \tag{5}$$

Exploring the dependence of γ on R_M has been the subject of extensive research. For sufficiently small R_M, the diffusion term in Eq. (1) will dominate, and magnetic energy will decrease exponentially with decay rate $-\gamma \sim U k_u R_M^{-1}$ (for $R_M \ll 1$). As R_M is increased, the stretching term becomes important, and above a critical value, a flow can become an effective dynamo ($\gamma > 0$). This value of R_M will be referred to as the critical magnetic Reynolds number and will be denoted as R_{MC}. Finding the flow that minimizes R_{MC} is of importance for laboratory dynamo experiments on account of R_M being an increasing function of power consumption, which is an increasing function of cost.

For large values of the magnetic Reynolds number, the problem becomes increasingly complex with the number of degrees of freedom involved increasing, such as $R_M^{3/2}$. Due to this complexity, there is no general analytical way to estimate the growth rate of a dynamo (with the exception of some special cases). Nonetheless, antidynamo theorems [16,17], developed in the last century, and upper bounds on the growth rate [18–21] have been proven useful in excluding certain classes of flows from giving dynamo action or restricting the scaling of γ with R_M. From the antidynamo theorems, two important results that are relevant in this paper are mentioned here.

First, flows with only two nonzero components of the velocity field cannot result in a dynamo for any value of R_M [17]. Thus, for these flows, there is no critical Reynolds number. In the present paper, we will refer to these flows as two-dimensional (2D) flows (even if there is spatial dependence in the third direction).

Second, time independent flows, for which all three components of the velocity (u_x, u_y, u_z) are nonzero but only depend on two of the spatial components (say, x, y), can result in a dynamo, but due to the absence of chaotic flow lines, the dynamo growth rate will tend to a nonpositive value as R_M tends to infinity [22,23]. For these flows, thus, it is expected that

$$\gamma = o(1)U k_u, \tag{6}$$

where the symbol $o(1)$ stands for smaller than order 1. This dependence, however, can be a very slowly decreasing function of R_M [24]. These flows are referred to as $2\frac{1}{2}$-dimensional flows, and the resulting dynamo is referred to as a slow dynamo.

However, besides these classes of flows, typical three-dimensional flows, with a complex streamline topology, are expected to be dynamos at infinitely large R_M [25]. For such flows, the growth rate will approach a value that will depend only on the amplitude, length scale, and structure of the velocity field and not on the magnetic diffusion η, i.e.,

$$\gamma = O(1)U k_u, \tag{7}$$

where the symbol $O(1)$ stands for same order as 1. Such flows, for which the dynamo growth rate tends to a positive value as R_M tends to infinity, are called fast dynamo flows.

With these restrictions in mind, a definition of an optimal flow can be given. The choice of optimization, of course, will depend on the application in mind. For example, an optimal flow can be based on R_{MC} or on γ leading to different answers. Here, we will be restricted to the following questions: Given a family of flows of fixed velocity amplitude U and length scale k_u, (i) which member has the smallest critical magnetic Reynolds number R_{MC}, (ii) given R_M, which member has the largest growth rate $\gamma/(U k_u)$, and finally, (iii) which flow leads to the largest growth rate in the limit $R_M \to \infty$. As shown later, these questions do not have the same answer.

Finally, we need to restrict the family of flows that is going to be investigated. Since the estimate of the growth rate γ and R_{MC} needs to be performed numerically, addressing the questions above for a large family of flows is formidable even for present day computing. Then, it is preferable to be restricted to smaller families that, however, are good candidates for fast dynamo action based on their properties.

For a fast dynamo, the role of Lagrangian chaos and the helicity of the flow have been emphasized as important ingredients. Lagrangian chaos, the exponential stretching of fluid elements, is a necessary ingredient for a fast dynamo [22,23]. However, it is not sufficient. Time dependent 2D flows can result in chaos (positive Lyapunov exponent) but can be excluded from dynamo flows based on the first antidynamo theorem mentioned here. The reason for this behavior is that the flow is required not only to exponentially stretch the magnetic field lines, but also to arrange them in a constructive way so that, when they are brought arbitrarily close, they can survive the effect of diffusion. A quantitative measure of these effects can be obtained by multiplying Eq. (1) by $\mathbf{b}$, space averaging, dividing by $\langle \mathbf{b}^2 \rangle$, and finally, by using Eq. (2) to obtain

$$\gamma + \partial_t \ln[\langle \tilde{\mathbf{b}}^2 \rangle] = \frac{\langle \mathbf{b} \cdot (\nabla \mathbf{u}) \mathbf{b} \rangle}{\langle \mathbf{b}^2 \rangle} - \eta \frac{\langle (\nabla \mathbf{b})^2 \rangle}{\langle \mathbf{b}^2 \rangle}. \tag{8}$$

Performing a time average and using the fact that $\tilde{\mathbf{b}}$ is bounded, the last equation can be written as

$$\gamma = \gamma_s - \gamma_d, \tag{9}$$

where γ_s is the time average of the first term on the right hand side of Eq. (8) and expresses the injection rate of energy by stretching, while γ_d is the time average of the second term

and expresses the dissipation rate. A constructive flow then has large γ_s and small γ_d. This can be obtained by the stretch-twist-fold mechanism [26] that aligns the stretched magnetic field lines so that they have the same orientation. It is expected to be achieved most efficiently if the flow is helical.

Helicity is the other ingredient that is expected to improve dynamo action. It is a measure of the lack of reflection symmetry of the flow [2] and is related to the linking number of the flow lines. Although, in general, it is not necessary [27], it has been thought to improve dynamo action, and it is required for α^2 dynamos [28–30]. It is also considered important for the generation of the large-scale magnetic fields that are observed in the universe [31–34].

In this paper, we are going to restrict ourselves to a family of flows that is both fully helical and is known to have chaotic flow lines, namely, the ABC flows. The ABC flows include a wide range of expected dynamo behaviors that covers 2D flows and slow and fast dynamos. Particular members of this family have been well studied for dynamo action, and this allows for a comparison with previous results. This choice is rather restrictive since it is not known *a priori* if the optimal dynamo flow belongs in the family of ABC flows. However, they provide a tractable set of flows to examine and a good starting guess.

The ABC flows are reviewed in detail in the next section.

III. THE ABC FAMILY

The ABC flow is named after Arnold [8], Beltrami [9], and Childress [10] and is explicitly given by

$$
\begin{aligned}
u_x &= A\,\sin(k_u z) + B\,\cos(k_u y),\\
u_y &= C\,\sin(k_u x) + A\,\cos(k_u z),\\
u_z &= B\,\sin(k_u y) + C\,\cos(k_u x).
\end{aligned}
\tag{10}
$$

It is an incompressible periodic flow with four independent parameters A, B, C, and k_u. The flow has the property,

$$
\mathbf{w} = \nabla \times \mathbf{u} = k_u \mathbf{u},
\tag{11}
$$

for all values of A,B,C,k_u. As a result, it is an exact solution of the Euler equations. It has been studied both for its properties as a solution of the Euler equation, its relation to chaos [35–37] and for dynamo instability [38–41] but only for limited values of the parameters. Here, it is attempted to uncover the dynamo properties for the whole family.

With no loss of generality, we can restrict ourselves only to flows of fixed wave number k_u and fixed velocity amplitude $U = \sqrt{A^2 + B^2 + C^2}$. With this restriction and property (11), the energy of the flow $E = \frac{1}{2}U^2$, the enstrophy of the flow,

$$
\Omega = \tfrac{1}{2}\langle \mathbf{w}\cdot\mathbf{w}\rangle = \tfrac{1}{2}k_u^2 U^2,
\tag{12}
$$

and the helicity H of the flow,

$$
H = \tfrac{1}{2}\langle \mathbf{w}\cdot\mathbf{u}\rangle = \tfrac{1}{2}k_u U^2
\tag{13}
$$

have a fixed value.

For fixed kinetic energy, the parameters A,B,C live on the surface of a sphere of radius U and can be parametrized using the spherical coordinates ψ,ϕ,

$$
A = U\,\cos(\psi),
\tag{14}
$$

$$
B = U\,\sin(\psi)\cos(\phi),
\tag{15}
$$

$$
C = U\,\sin(\psi)\sin(\phi).
\tag{16}
$$

Using the symmetries of the ABC flow (see Refs. [36,39]), we can restrict the examined parameter space. The flow is invariant under the transformations,

$$
[A,z] \to [-A, z - \pi/k_u],
\tag{17}
$$

$$
[B,y] \to [-B, y - \pi/k_u],
\tag{18}
$$

and

$$
[C,x] \to [-C, x - \pi/k_u].
\tag{19}
$$

These symmetries allow restricting the investigation to only positive values of A, B, and C and, thus, reduce the examined parameter space to the range $[0,\pi/2]$ for both angles ϕ and ψ. Since there is no preferred direction between (x,y,z), the growth rate is also going to be independent under permutations, e.g., $(B,C) \to (C,B)$. More precisely, the flow is invariant under the transformations,

$$
\begin{bmatrix} (A,B,C) \\ (x,y,z) \end{bmatrix} \to \begin{bmatrix} (A,C,B) \\ \left(\dfrac{3\pi}{2k_u} - y, \dfrac{3\pi}{2k_u} - x, \dfrac{3\pi}{2k_u} - z \right) \end{bmatrix},
\tag{20}
$$

$$
\begin{bmatrix} (A,B,C) \\ (x,y,z) \end{bmatrix} \to \begin{bmatrix} (B,A,C) \\ \left(\dfrac{3\pi}{2k_u} - x, \dfrac{3\pi}{2k_u} - z, \dfrac{3\pi}{2k_u} - y \right) \end{bmatrix},
\tag{21}
$$

$$
\begin{bmatrix} (A,B,C) \\ (x,y,z) \end{bmatrix} \to \begin{bmatrix} (C,B,A) \\ \left(\dfrac{3\pi}{2k_u} - z, \dfrac{3\pi}{2k_u} - y, \dfrac{3\pi}{2k_u} - x \right) \end{bmatrix}.
\tag{22}
$$

These symmetries allow interchanging the values of any of the three parameters A,B,C, thus, a single numerical simulation gives the growth rate for six points in the parameter range $\psi \in [0,\pi/2]$ and $\phi \in [0,\pi/2]$. This additional information was used to increase the number of measured values. Finally, the change $k \to -k$ changes the sign of the helicity of the flow. This change, however, does not alter the resulting growth rate of the dynamo. Thus, only positive values of k are considered.

Depending on the values of the parameters A,B,C, the flow can have eight stagnation points where all three components of the velocity are zero. These points exist only if the square of each the parameters A,B,C is smaller than the sum of the square of the other two [36] (i.e., their squares can form a triangle). The importance of the existence or absence of stagnation points was emphasized in Ref. [15]. It was noticed that the developed magnetic structures changed from from cigar-shaped, in the presence of stagnation points, to ribbon-shaped in their absence.

Figure 1 demonstrates the examined parameter space in the spherical coordinates (ψ,ϕ). Some of the points in this graph represent flows of special significance that are described in what follows. For $(\psi = \pi/2, \phi = \pi/2)$, $(\psi = \pi/2, \phi = 0)$, and $(\psi = 0)$, two of the three parameters A,B,C are zero $(A = B = 0$, $A = C = 0$, and $B = C = 0$, respectively). The flow corresponding to these points is 2D, and thus, there is no dynamo, $\gamma < 0$.
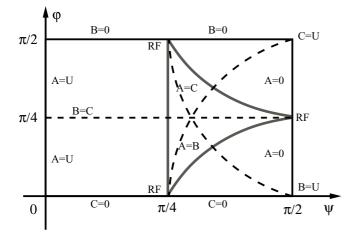
FIG. 1. A sketch of the parameter space for the ABC family of flows. RF marks the location of the Roberts Flow. The dashed lines indicate the location where two of the three parameters (A,B,C) are equal, and at their intersection, is the 1:1:1 flow. The gray lines enclose the region where stagnation points exist.

For $(\psi = \pi/2)$, we have $A = 0$, for $(\phi = \pi/2)$, we have $B = 0$, and for $(\phi = 0)$, we have $C = 0$; for these values of (ψ, ϕ) for which one of the three parameters A, B, C is zero, the resulting flow is a $2\frac{1}{2}$-dimensional flow and, thus, a slow dynamo. The RF is a special flow in this subset for which the two nonzero parameters are equal. It has been studied for slow dynamo action in Refs. [11,12,24]. It corresponds to the values $(\psi = \pi/2, \phi = \pi/4)$, $(\psi = \pi/4, \phi = \pi/2)$, and $(\psi = \pi/4, \phi = 0)$, and in Fig. 1, it is marked as RF.

Flows that have two of the three parameters equal have additional symmetries and as will be shown in Sec. IV, they are important. These flows are located along the line $\phi = \pi/4$ for $B = C$, the line $\psi = \arctan[1/\cos(\phi)]$ for $A = B$, and the line $\psi = \arctan[1/\sin(\phi)]$ for $A = C$. These lines are shown by dashed lines in Fig. 1 and divide the space in six compartments. Each of these compartments is equivalent to the others due to the symmetries in Eqs. (20)–(22) . Thus, each of these compartments will have the same number of maxima and minima of the growth rate.

When all three parameters are equal, $A = B = C$, the flow has the largest number of symmetries. This flow is the most studied one in the literature, and it is going to be referred to as the 1:1:1 flow. It is obtained for $[\phi = \pi/4, \psi = \arctan(\sqrt{2})]$ and is located at the intersection of the dashed lines in the diagram.

Finally, the region of the parameter space for which the ABC flow has stagnation points is enclosed by the gray lines in Fig. 1.

ABC flows are known to be chaotic [35–40]. Finite time Lyapunov exponents provide a measure of chaos [42]. The finite time Lyapunov exponent $\lambda_\tau(x_0)$, for a point x_0, is defined as

$$\lambda_\tau(x_0) = \frac{1}{\tau} \ln \left[\frac{|\delta \mathbf{x}(\tau)|}{|\delta \mathbf{x}(0)|} \right], \tag{23}$$

where $|\delta \mathbf{x}(\tau)|$ is the distance of two particles that, at time $\tau = 0$, were placed infinitesimally close to x_0. If the flow is not ergodic, not all initial points x_0 of a chaotic flow lead to
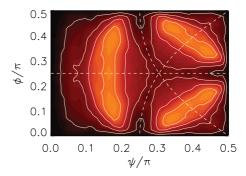

FIG. 2. (Color online) Color-scale plot of the finite time Lyapunov exponent λ_τ in the ψ, ϕ plane. Bright colors imply large values of the exponents, while black implies zero or close to zero values. The contour lines correspond to the levels $\lambda_\tau = 0.02, 0.04, 0.06,$ and 0.08. The time of integration was $\tau = 2 \times 10^4$.

$\lambda_\tau > 0$. Thus, to measure λ_τ of the flow, an ensemble of initial points x_0 needs to be considered out of which only those that belong to the chaotic subset will lead to $\lambda_\tau > 0$. Here, $\lambda_\tau(x_0)$ was calculated for the ABC flows and for 8000 initial positions x_0 distributed uniformly in the domain $[0, 2\pi)^3$. The distribution function of the measured Lyapunov exponents was constructed, and λ_τ of the chaotic subset was determined as the location of the peak in the distribution function.

In Fig. 2, a color-scale plot of λ_τ is shown for the (ψ, ϕ) plane, and in Fig. 3, the finite time Lyapunov exponents are shown for $\phi = \pi/4$. It is worth noting that the λ_τ of the most symmetric flow 1:1:1 is a local minimum (see also Ref. [40]), while the largest values of λ_τ appear for $(\phi = \pi/4, \psi \simeq 0.155\pi)$ and for $(\phi \simeq 0.12\pi, \psi \simeq 0.16\pi)$ and the equivalent points by symmetry.

IV. DYNAMO RESULTS

The advection diffusion equation (1) was solved in a triple periodic domain of size $L = 2\pi$ using a standard pseudospectral method and a third order in time Runge-Kutta [43,44]. The resolution used varied from 32^3 grid points for small values of $R_M (\lesssim 20)$ up to 256^3 for the largest values $R_M \gtrsim 500$. Each run was evolved for a sufficiently long time
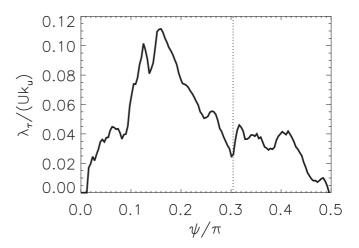

FIG. 3. Plot of the finite time Lyapunov exponent λ_τ for $\phi = \pi/4$. The time of integration was $\tau = 10^6$.

until a clear exponential increase in the magnetic energy was observed, and the growth rate was calculated by fitting.

The last parameter that needs to be defined is the ratio of the box size L over which the magnetic field is allowed to evolve in, to the period of the velocity field $2\pi/k_u$. Due to the periodicity, the product $k_u L$ can only be integer multiples of 2π. Here, we are going to examine two cases $k_u L = 2\pi$ where the two lengths are equal and $k_u L = 4\pi$ where the magnetic field can evolve on a larger scale.

A. ABC, $k_u L = 2\pi$

First, the case $k_u L = 2\pi$ is presented. In Fig. 4, color-scale images of the measured growth rate are shown for six different values of R_M. Each figure corresponds to 200 different dynamo simulations. By using 20 different values of ψ in the range $[0,\pi/2]$ and 10 for ϕ in the range $[0,\pi/4]$, the symmetries in Eqs. (20)–(22) were used to fill in the values of the growth rate on the whole domain and on a denser grid. In each panel, bright colors correspond to larger growth rates. The thick white lines show the location of zero growth rate. The thin black lines indicate where the growth rate is $0.05Uk_u$. The dashed black lines, as in Fig. 1, show the location on which two of the three parameters A,B,C are equal. Finally, it is noted that the simulations in these runs were performed on 32^3 and 64^3 grid-point meshes.

As R_M is increased, the first flows that result in positive growth rates are the ones with two of the three parameters equal, while the third is equal to zero. This can be seen in the top left panel of Fig. 4 for $R_M = 10$ where most of the
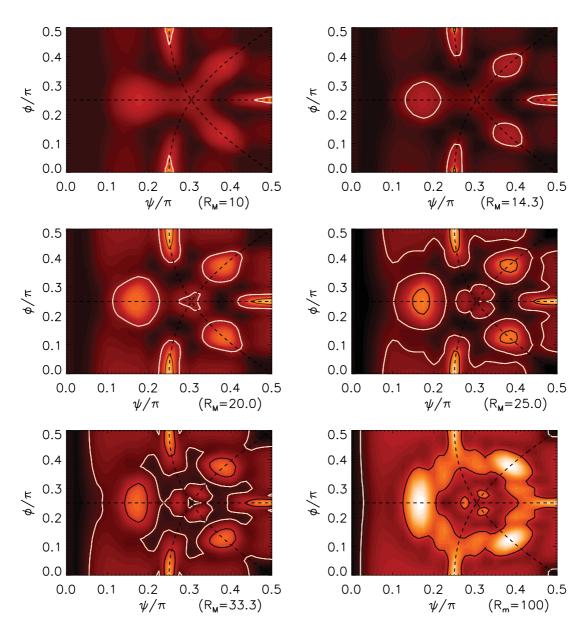

FIG. 4. (Color online) Color-scale images of the growth rate in the ψ,ϕ plane for $k_u L = 2\pi$ and for six different magnetic Reynolds numbers. Bright colors indicate larger growth rates. The thick white lines are the contour lines' zero growth rate. Thin black lines are the contour lines of growth rate $\gamma = 0.05Uk_u$. The dashed lines (as in Fig. 1) indicate the location at which two of the three parameters A,B,C are equal.

parameter domain has a negative growth rate except the small bright regions at the end of the dashed lines. These flows correspond to a RF and are slow dynamos as discussed in the previous section. Thus, although they are slow, at small R_M, they are the most efficient at producing a dynamo (i.e., the fastest).

The next flows that become unstable are the flows for which two of the three parameters are equal but smaller than the third. Thus, they lie on the dashed lines in the graph opposite the RF. This can be seen in the right top panel of Fig. 4 that shows the growth rate for $R_M = 14.3$. In terms of the angles, they correspond to the values ($\psi \simeq 0.17\pi$, $\phi = \pi/4$) and ($\psi \simeq 0.38\pi$, $\phi = \pi/4 \pm 0.12\pi$). The exact location of these new maxima is shifting slowly away from the center as the magnetic Reynolds number is increased. Note that this flow is very close to the flow for which the maxima for the Lyapunov exponents in Figs. 2 and 3 were found. It is also close to the flow $A = 5$, $B = C = 2$ that was investigated in detail in Ref. [15]; for this reason, this flow is going to be referred to as the 5:2:2 flow. At this value of the Reynolds number, the RF is still the fastest dynamo in the family.

As the magnetic Reynolds number is increased further, the most symmetric flow 1:1:1 also results in a dynamo. This is shown in the middle left panel of Fig. 4 for $R_M = 20$. At this value of R_M, the 1:1:1 is a local maximum, but with a smaller growth rate than the 5:2:2 flow and smaller than the RF that is still the fastest.

As R_M is increased further, the 1:1:1 flow stops being a local maximum and transitions to a third-order saddle point (monkey saddle point). This can be seen in the middle right panel for which $R_M = 25$. The local maximum of the 1:1:1 flow, which was present at $R_M = 20$, splits into three local maxima that move along the dashed lines away from the 1:1:1 case whose growth rate has decreased. The growth rate for the 5:2:2 flow and the RF continues to increase.

For $R_M = 33.3$ (shown in the bottom left panel), the three local maxima that were initially located close to the 1:1:1 flow have moved sufficiently away that the 1:1:1 flow stops being a dynamo. This corresponds to the no-dynamo window that was observed early on in Ref. [38].

After a further increase in R_M, the 1:1:1 flow becomes a dynamo again (although not a local maximum anymore but still a saddle point). For $R_M = 100$ shown in the bottom right panel, most of the parameter space results in dynamo action, with the only exception being where the small areas are close to the 2D flows ($\psi = \pi/2$, $\phi = \pi/2$), ($\psi = \pi/2$, $\phi = 0$), and ($\psi = 0$). The growth rate of the RF has started to decrease, and the fastest dynamo is given by the 5:2:2 flow. At this value of R_M, the topography of the growth rate in the parameter space has become much more complex, with new local maxima appearing between the RF and the 5:2:2 flow. This increase in complexity with R_M has also been observed in $2\frac{1}{2}$-dimensional flows parametrized by the wave number in the invariant direction [14].

For larger values of R_M, grids larger than 64^3 are needed, and it is computationally too expensive to cover the whole parameter domain. Instead, the investigation will be limited to flows that lie along the dashed lines where most of the maxima are located. In Fig. 5, we show the growth rate for three different values of the magnetic Reynolds number with
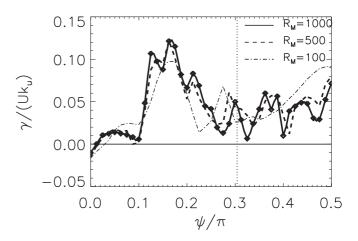

FIG. 5. Nondimensional growth rate as a function of ψ for $\phi = \pi/4$ and for three different magnetic Reynolds numbers. The vertical dotted line marks the location of the 1:1:1 flow.

the smallest value being equal to the value used in the last panel of Fig. 4. The 5:2:2 flow results in the fastest dynamo at the largest value of $R_M = 1000$. At this value of R_M, the 5:2:2 peak has moved to $\psi \simeq 0.16\pi$. Furthermore, for $R_M > 500$, two new local maxima appear close to the 5:2:2 flow for slightly smaller and slightly larger values of ψ. The local maximum, which, at small values of R_M, was located at the 1:1:1 flow, appears to return close to the 1:1:1 point, and thus, the most symmetric flow comes close to a local maximum again. Finally, the slow decrease in the growth rate of the RF can be observed.

In Fig. 6, the two rates γ_s (dashed line, triangles) and γ_d (solid line, diamonds), defined in Eq. (9), are shown for the largest examined $R_M = 1000$. The difference between the two curves gives the growth rate. The ratio of the two curves shows the percentage of the injected energy that is dissipated. Thus, a constructive flow (in the sense that it aligns magnetic field lines pointing in the same direction) is expected to have a small value of γ_d compared to γ_s. The flows close to the 5:2:2 flow ($\psi = 0.16\pi$) that have the largest growth rates are more efficient not only due to the larger stretching rate γ_s that does not vary a lot, but also due to the relatively small value of γ_d. In
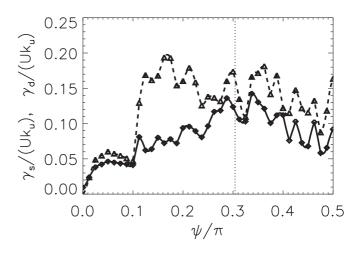

FIG. 6. The rates γ_s (dashed line, triangles) and γ_d (solid line, diamonds) defined in Eq. (9) for the $k_u L = 2\pi$ case and for $R_M = 1000$. The vertical dotted line marks the location of the 1:1:1 flow.

the range $\psi = 0.1\pi$ to $\psi = 0.25\pi$, half of the energy injected by stretching goes to magnetic field amplification. For values of ψ out of this range, only a small fraction of the injected energy goes to field amplification while the rest goes to the small scales where it is dissipated.

Beyond the $\phi = \pi/4$ symmetry line, other local maxima of the growth rate were detected, although it was not feasible to cover the entire parameter space. Here, it is just mentioned that a local maximum was observed at ($\psi = 0.2\pi, \phi = 0.1\pi$) with a growth rate close to the 5:2:2 flow $\gamma \simeq 0.12$.

B. ABC $kL = 4\pi$

The case $k_u L = 4\pi$ is examined in this section. Despite the fact that the flow is the same as in the $k_u L = 2\pi$ case, the results are different due to the additional space in which the magnetic field is allowed to evolve. The extra space gives rise to new modes that can develop with different growth rates. Although the modes of the $k_u L = 2\pi$ case still are present and grow at the same rate, they are not necessarily the fastest. Considering that, in a numerical simulation, only the fastest growing mode is observed, in the $k_u L = 4\pi$ case, the observed mode will then be, at least, as fast as the $k_u L = 2\pi$ case.

As before, the first flows that result in a dynamo are the slow dynamos of the RF for which two of the three parameters A, B, C are equal and the third is zero. This case is shown in the right panel of Fig. 7 for $R_M = 2.5$. Note that, in this case, the dynamo instability appears at much smaller values of R_M. It is also remarkable that the mode, whose growth rate peaks

for the RF, appears to continuously extend all the way to the 1:1:1 flow that is a saddle point at this stage.

As R_M increases further, the 1:1:1 flow becomes a dynamo whose growth rate is a local maximum in the (ψ, ϕ) plane. This is shown in the top right panel of Fig. 7 that corresponds to $R_M = 10$. Note also that this is contrary to the $k_u L = 2\pi$ case for which the 5:2:2 flow was the second flow to result in a dynamo. In the $k_u L = 4\pi$ case and for this value of R_M, there is no observed local maximum close to the 5:2:2 flow.

As R_M is further increased, the growth rate of the 1:1:1 flow is increased. At $R_M = 25$, the 1:1:1 flow exceeds the RF in growth rate, and it is the fastest dynamo for all ABC flows. This can be seen in the bottom left panel of Fig. 7. This is somehow surprising since this flow was never the fastest in the $k_u L = 2\pi$ case.

At even larger R_M, however, the growth rate of the 1:1:1 ceases to increase while the 5:2:2 becomes a local maximum and obtains comparable values with the 1:1:1 flow. This is shown in the bottom right panel of Fig. 7.

The growth rate for larger values of R_M was calculated only along the symmetry line $\phi = \pi/4$. It is shown as a function of ψ and for three different values of R_M in Fig. 8. The smallest value of R_M corresponds to the results of the bottom right panel of Fig. 7. As the magnetic Reynolds number is increased, the growth rate of the 1:1:1 flow is decreased while, at the same time, the growth rate of the 5:2:2 flow is increased. At the largest examined value of R_M, the fastest dynamo is given by the 5:2:2 flow with a growth rate $\gamma/(k_u U) = 0.16$, which is larger than its growth rate in the $k_u L = 2\pi$ case.
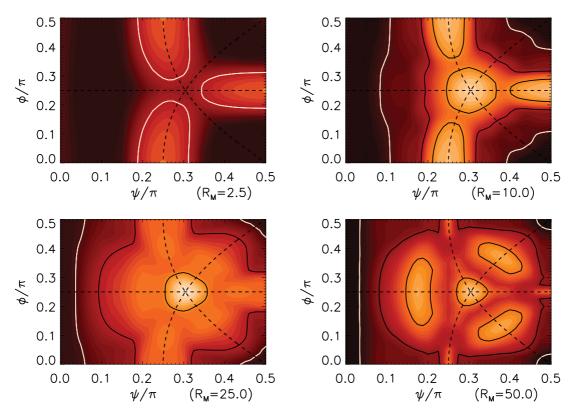

FIG. 7. (Color online) Color-scale images of the growth rate in the ψ, ϕ plane for $k_u L = 4\pi$ and for four different magnetic Reynolds numbers. Bright colors indicate larger growth rates. The thick white lines are the contour lines' zero growth rate. Thin black lines are the contour lines of growth rate $\gamma = 0.05 U k_u$ and $\gamma = 0.1 U k_u$. The dashed lines (as in Fig. 4) show the location at which two of the three parameters A, B, C are equal.
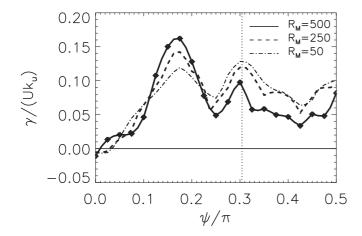
FIG. 8. The growth rate as a function of ψ and for $\phi = -\pi/4$ for $k_u L = 4\pi$ and three different Reynolds numbers. The vertical dotted line marks the location of the 1:1:1 flow.

As in the previous section, in Fig. 9, we plot the two growth rates γ_s (dashed line, triangles) and γ_d (solid line, diamonds) for $R_M = 500$. In this case, the the ability of the 5:2:2 flow to align field lines reducing dissipation is even more pronounced. Only one fifth of the injected energy is cascading to the dissipated scales while the rest is going in the amplification of the magnetic field. Unlike the $k_u L = 2\pi$ case, the 1:1:1 flow is also being more constructive with less than half of the energy going to dissipation.

It is also worth comparing the general behavior of the growth rate with the results in the previous section. Although the fastest dynamo flows appear at the same location, their growth rates are different, thus, it is not the same dynamo modes that are observed in the two cases. Also, in the $k_u L = 4\pi$ case, the dependence of the growth rate on the flow at the large R_M is less complex than in the $k_u L = 2\pi$ case with less local maxima and a smoother, in general, behavior. These differences indicate that the box size plays an important role in the dynamo behavior.

V. SUMMARY AND CONCLUSIONS

In this paper, the entire family of ABC flows was examined for dynamo action. The dynamo growth rate was calculated as a function of the magnetic Reynolds number R_M and for two length scales $k_u L = 2\pi$ and $k_u L = 4\pi$. The questions
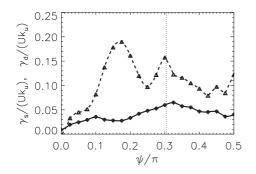

FIG. 9. The rates γ_s (dashed line, triangles) and γ_d (solid line, diamonds) defined in Eq. (9) for the $k_u L = 4\pi$ case and for $R_M = 500$. The dotted vertical line marks the location of the 1:1:1 flow.

that this paper was attempting to answer were: (i) which flow has the smallest critical magnetic Reynolds number R_{MC}, (ii) given R_M, which flow has the largest growth rate $\gamma/(U k_u)$, and (iii) which flow leads to the largest growth rate in the limit $R_M \to \infty$. Although these questions can be posed for a larger family of flows, the ABC flows constitute a first step in obtaining some understanding.

For this, perhaps, restrictive family of flows, the answer to the first question is a simple one: The RF results in a dynamo for the smallest value of R_M. This is true for both the $k_u L = 2\pi$ and the $k_u L = 4\pi$ cases. Thus, in small Reynolds numbers, a well organized flow can do much better than a rapidly stretching (chaotic) flow.

At larger Reynolds numbers, new dynamo modes became unstable, and a number of bifurcations are observed that lead to a complex topography of the growth rate. As R_M was increased, this complexity was further increased, and more local maxima appeared. This was particularly true for the $k_u L = 2\pi$ case, while for the $k_u L = 4\pi$ case, a smoother behavior was observed.

Inspecting the growth rate for a large number of flows as performed in this paper also gives a wider perspective on the dependence of magnetic eigenmodes of the flow on R_M. Some of the observed dynamo modes of a given flow can be related (by continuous transform) to the modes of different flows. For example, for small values of R_M, the slowest decaying mode of the 1:1:1 flow is related to the dynamo mode of the RF (see Fig. 7 top left panel). Thus, the various bifurcations that can be observed by looking at the growth rate of a single flow can be interpreted as shifting or enlargement of local maxima in this wider point of view. The no-dynamo window of the 1:1:1 flow is such an example, which is the outcome of splitting and shifting of the initial maximum at the 1:1:1 point.

Finally, for relative large R_M, the 5:2:2 flow ($\psi \simeq 0.16\pi$, $\phi = \pi/4$) has the fastest growing mode (from the examined flows) in both cases ($k_u L = 2\pi$ and $k_u L = 4\pi$). However, if this continues to be true, even larger values of the magnetic Reynolds number cannot be concluded from the present data. $R_M = 1000$ is still far from the $R_M \to \infty$ limit as can be seen from the finite value of the growth rate of the RF, which is a slow dynamo. Furthermore, as noted at the end of Sec. IV A, flows that were not on the $\phi = \pi/4$ symmetry line were found with growth rates similar to the 5:2:2 flow. The increased complexity of the growth rate as R_M increases makes it harder to estimate the fastest dynamo flow. If this continues, then the location of the fastest flow in the (ψ, ϕ) plane might not converge to a single point in the limit $R_M \to \infty$ and question (iii) might not even have an answer.

On the other hand, the Lyapunov exponents, whose value does not depend on R_M, do show some clear maxima, which gives hope that a fastest dynamo flow in the $R_M \to \infty$ limit exists. However, although a correlation of the growth rate with the Lyapunov exponents is observed, it is definitely not sufficient to explain the dependence of the observed growth rates, at least, not at the examined values of R_M. In particular, it is observed that the flow with the largest growth rate is close to the flow with the largest Lyapunov exponent. Nevertheless, the general dependence of the growth rate and of the Lyapunov exponent on the flow is quite different, with local maxima appearing at different locations.

In addition, it was found that the 5:2:2 flow that leads to the fastest growing mode besides having a large stretching rate was also very efficient at organizing the magnetic field lines as to minimize the magnetic energy dissipation. Furthermore, at the examined values of R_M, the $k_u L = 2\pi$ and the $k_u L = 4\pi$ cases showed significant differences, although the magnetic field lines were advected by the same flows. Thus, the growth rate cannot be determined by the stretching statistics of the flow alone. If these differences cease to exist at larger R_M is a question for future papers.

Besides investigating larger R_M, there are many other obvious extensions of this paper. First, it would be interesting to extend these results to a larger family of flows, which also includes nonhelical flows. Harmonic velocity fields could be such a generalization. The fastest dynamo flow in such a large family could possibly be obtained by an optimization routine.

A differently oriented approach would consider turbulent dynamos. In this case, instead of prescribing the flow, a body force would be prescribed, and the flow would be allowed to evolve dynamically. In such a study, different limits of the kinetic Reynolds number Re would lead to different results. In the limit $1 \ll \mathrm{Re} \ll R_M$, dynamo growth rates depend on the small velocity scales and are possibly universal. In the other limit $1 \ll R_M \ll \mathrm{Re}$, it has been shown that the large-scale flow plays an important role especially for R_M near its threshold value [45–47].

Finally, the properties of dynamos beyond the linear regime, where our understanding is much more limited, is also a problem of considerable interest. At the nonlinear stage, both the saturation levels of the magnetic energy and the involved length scales (large- or small-scale dynamo) depend strongly on the large-scale properties of the flow. Thus, a systematic study of a large number of flows can be helpful in that respect.

These issues are going to be pursued in another paper.

ACKNOWLEDGMENTS

[1] Y. B. Zeldovich, A. A. Ruzmaikin, and A. A. Sokoloff, *Magnetic Fields in Astrophysics* (Gordon and Breach, New York, 1990).

[2] H. K. Moffatt, *Magnetic Field Generation in Electrically Conducting Fluids* (Cambridge University Press, Cambridge, UK, 1978).

[3] A. Gailitis, O. Lielausis, E. Platacis, S. Dement'ev, A. Cifersons, G. Gerbeth, T. Gundrum, F. Stefani, M. Christen, and G. Will, Phys. Rev. Lett. **86**, 3024 (2001).

[4] R. Stieglitz and U. Müller, Phys. Fluids **13**, 561 (2001).

[5] R. Monchaux, M. Berhanu, M. Bourgoin, M. Moulin, P. Odier, J. F. Pinton, R. Volk, S. Fauve, N. Mordant, F. Pétrélis, A. Chiffaudel, F. Daviaud, B. Dubrulle, C. Gasquet, L. Marie, and F. Ravelet, Phys. Rev. Lett. **98**, 044502 (2007).

[6] F. Ravelet, A. Chiffaudel, F. Daviaud, and J. Leorat, Phys. Fluids **17**, 117104 (2005).

[7] Y. B. Ponomarenko, Zh. Prikl. Mekh. and Tekh. Fiz. (USSR) **6**, 47 (1973).

[8] V. I. Arnold, C. R. Acad. Sci. Paris **17**, 261 (1965).

[9] E. Beltrami, Opera Matematiche **4**, 304 (1889).

[10] S. Childress, J. Math. Phys. **11**, 3063 (1970).

[11] G. O. Roberts, Phil. Trans. R. Soc. Lond. A **266**, 535 (1970).

[12] G. O. Roberts, Phil. Trans. R. Soc. Lond. A **271**, 411 (1972).

[13] Y. Ponty, P. D. Mininni, J.-P. Laval, A. Alexakis, J. Baerenzung, F. Daviaud, B. Dubrulle, J. F. Pinton, H. Politano, and A. Pouquet, C. R. Phys. **9**, 749 (2008).

[14] A. Couvrvoisier, A. D. Gilbert, and Y. Ponty, Geophys. Astrophys. Fluid Dyn. **99**, 413 (2005).

[15] V. Archontis, S. B. F. Dorch, and A. Nordlund, Astron. Astrophys. **472**, 715 (2007).

[16] T. G. Cowling, Mon. Not. R. Astron. Soc. **140**, 39 (2001).

[17] Y. B. Zeldovich, Sov. Phys. JETP **4**, 460 (1957).

[18] G. Backus, Ann. Phys. **4**, 372 (1958).

[19] S. Childress, in *Lecture Notes* (Département Mécanique de la Faculté des Sciences, Paris, 1969).

[20] M. R. E. Proctor, Geophys. Astrophys. Fluid Dyn. **14**, 127 (1979).

[21] M. R. E. Proctor, Geophys. Astrophys. Fluid Dyn. **98**, 235 (2004).

[22] S. Friedlander and M. M. Vishik, Chaos **1**, 198 (1991).

[23] M. M. Vishik, Geophys. Astrophys. Fluid Dyn. **48**, 151 (1989).

[24] A. M. Soward, J. Fluid Mech. **180**, 267 (1987).

[25] J. M. Finn and E. Ott, Phys. Fluids **31**, 2992 (1988).

[26] S. Childress and A. D. Gilbert, in *Stretch, Twist, Fold: The Fast Dynamo*, Lecture Notes in Physics Monographs (Springer, Berlin, 1995).

[27] D. W. Hughes, F. Cattaneo, and K. Eun-Jin, Phys. Lett. A **223**, 167 (1996).

[28] E. N. Parker, Astrophys. J. **122**, 293 (1955).

[29] S. Braginsky, JETP **20**, 726 (1964).

[30] M. Steenbeck, F. Krause, and K. Radler, Z. Naturforsch. **21**, 369 (1966).

[31] M. Meneguzzi, U. Frisch, and A. Pouquet, Phys. Rev. Lett. **47**, 1060 (1981).

[32] A. Brandenburg, Astrophys. J. **550**, 824 (2001).

[33] E. T. Vishniac and J. Cho, Astrophys. J. **550**, 752 (2001).

[34] A. Alexakis, P. D. Mininni, and A. Pouquet, Astrophys. J. **640**, 335 (2006).

[35] V. I. Arnold and E. I. Korkina, Vestn. Mosk. Univ., Ser. 1: Mat. Mekh. **3**, 43 (1983).

[36] T. Dombre, U. Frisch, J. M. Greene, M. Henon, A. Mehr, and A. M. Soward, J. Fluid Mech. **167**, 353 (1986).

[37] O. M. Podvigina and A. Pouquet, Physica D **75**, 471 (1983).

[38] D. J. Galloway and U. Frisch, Geophys. Astrophys. Fluid Dyn. **36**, 53 (1986).

[39] A. D. Gilbert, Philos. Trans. R. Soc. London, Ser. A **339**, 627 (1992).

[40] B. Galanti, P. L. Sulem, and A. Pouquet, Geophys. Astrophys. Fluid Dyn. **66**, 183 (1992).

[41] V. Archontis, S. B. F. Dorch, and A. Nordlund, Astron. Astrophys. **397**, 393 (2003).

[42] D. Ott, *Chaos in Dynamical Systems* (Cambridge University Press, Cambridge, UK, 1993).

[43] D. O. Gomez, P. D. Mininni, and P. Dmitruk, Adv. Space Res. **35**, 899 (2005).

[44] D. O. Gomez, P. D. Mininni, and P. Dmitruk, Phys. Scr., T **T116**, 123 (2005).

[45] Y. Ponty and F. Plunian, Phys. Rev. Lett. **106**, 154502 (2011).

[46] Y. Ponty, P. D. Minnini, D. C. Montgomery, J.-F. Pinton, H. Politano, and A. Pouquet, Phys. Rev. Lett. **94**, 164502 (2005).

[47] A. A. Schekochihin, N. E. L. Haugen, A. Brandenburg, S. C. Cowley, J. L. Maron, and J. C. McWilliams, Astrophys. J. **625**, L115 (2005).